

The studies on mechanisms and applications of gamma-typed iron-oxides suspensions

Varut Emudom

Department of Mechanical Engineering, College of Engineering, Rangsit University, Patumthani, 12000, Thailand
E-mail: varutama8008@gmail.comSubmitted 8 July 2014; accepted in final form 26 February 2015
Available online 15 June 2015

Abstract

Magnetized particle agglomerates (MPA) suspensions can be modeled as monodisperse suspensions of hard, magnetic spheres in a Newtonian continuous phase. The application of a magnetic field to the MPA suspensions causes the rearrangement of particles leading to a new structure. This structure has been observed to form under quiescent conditions and is described as consisting of chains or columns of particles spanning the gap of two diamagnetic parallel plates. Most fibrous aggregates still remain intact during shearing. This shear rate can be considered to be close to a critical value of 0.5 s^{-1} such that the fibrous structure can be strained or unstrained reversibly without any rupture of the fibrous structure. At shear rate higher than the critical value, most of columnar structures begin to break into small portions. Applications of magnetized particles are also investigated in which pipe flow experiments were performed using magnetized particles as additive agents to the flow medium. Pipe flow friction can be controlled using ferromagnetic materials in the form of gamma-typed iron oxides Fe_2O_3 . Substantial friction reduction can be achieved with appropriate choice of operating parameters. Friction in pipe flow could be reduced as much as 80% with optimal operating parameters such as particle size, mass concentration, intensity of magnetization, and Reynolds number. The approximate ranges can be, for the initial exploratory testing, 30-50 microns in particle diameter, 2% in mass concentration, 1000 Gauss (G) for initial magnetization of particles, and 60,000 to 100,000 in Reynolds number.

Keywords: magnetized particle agglomerates, Newtonian, diamagnetic, ferromagnetic, Reynolds number

บทคัดย่อ

ของผสมผงแม่เหล็กไฟฟ้าสามารถถูกเปรียบเทียบให้เป็นของผสมเนื้อเดียวกันระหว่างผงแม่เหล็กทรงกลมและของไหลนิวโตเนียน การที่จ่ายสนามแม่เหล็กไฟฟ้าให้กับของผสมแม่เหล็กไฟฟ้านั้นจะทำให้เกิดการเรียงตัวของผงแม่เหล็กเป็นโครงสร้างใหม่ ซึ่งโครงสร้างใหม่ของผงแม่เหล็กนี้เกิดขึ้นในของไหลที่ไม่เคลื่อนตัวและมีลักษณะเป็นลูกโซ่ของผงแม่เหล็กเรียงต่อกันเป็นเส้นๆระหว่างแผ่นระนาบสองแผ่นที่มีคุณสมบัติต้านทานต่อสนามแม่เหล็กไฟฟ้า ส่วนใหญ่แล้วเส้นหรือลูกโซ่ของผงแม่เหล็กจะไม่ถูกกระทบถ้ามีความเค้นเฉือนเกิดขึ้นในของไหล โดยที่อัตราความเค้นเฉือนจะต้องไม่เกินค่าวิกฤติประมาณ 0.5 s^{-1} ที่ค่านี้เส้นหรือลูกโซ่ของผงแม่เหล็กสามารถยืดตัวหรือหดตัวโดยไม่มีภาวะขาดหรือหักเกิดขึ้น ที่อัตราความเค้นเฉือนมากกว่าค่าวิกฤติเส้นหรือลูกโซ่ของผงแม่เหล็กเกือบทั้งหมดจะขาดออกจากกันเป็นชิ้นส่วนเล็กๆ การนำเอาประโยชน์ของผงแม่เหล็กไปใช้จะถูกทดลองกับการไหลในท่อ โดยที่ผงแม่เหล็กจะถูกผสมเข้ากับน้ำที่ใช้ในการไหล จากการทดลองความเสียดทานในท่อสามารถถูกควบคุมได้โดยการใส่ผงแม่เหล็กไฟฟ้าออกไซด์ชนิดแกมมา การลดลงอย่างมากของความเสียดทานในท่อนั้นสามารถทำได้โดยการเลือกค่าของการไหลที่เหมาะสม ความเสียดทานในท่อถูกลดลงได้ถึง 80% ถ้าค่าของการไหล เช่น ขนาดของผงแม่เหล็ก อัตราส่วนของผงแม่เหล็กในของผสม ความเข้มข้นของสนามแม่เหล็กไฟฟ้าและตัวเลขเรย์โนลด์ของการไหลถูกเลือกให้เหมาะสม ค่าที่ดีที่สุดในการลดความเสียดทานในท่อสำหรับการทดลองเบื้องต้นคือ ขนาดของผงแม่เหล็กประมาณ 30-50 ไมครอน อัตราส่วนของผงแม่เหล็กในของผสมอยู่ที่ 2% ความเข้มข้นของสนามแม่เหล็กไฟฟ้าอยู่ที่ค่า 1000 เกาส์ และตัวเลขเรย์โนลด์อยู่ระหว่าง 60,000 ถึง 100,000

คำสำคัญ: ผงแม่เหล็กไฟฟ้าออกไซด์, ของไหลนิวโตเนียน, อัตราความเค้นเฉือน, ความเสียดทาน, ตัวเลขเรย์โนลด์

1. Introduction

The structure in the MPA (magnetized particle agglomerates) suspensions changes rapidly upon the application of an external magnetic field. The applied magnetic field can cause a separation in phase from a homogeneous solid-liquid suspension to solid state and liquid state. The apparent solid

state is due to the formation of elongated aggregates of magnetic particles which are aligned parallel to the magnetic field. Typical MPA suspensions contain a disperse phase of ferromagnetic materials with volume fractions in the range of 1% - 25% (Rosensweig, 2006). The ferromagnetic materials are in the form of iron oxides Fe_2O_3 (type Gamma)

or Fe_3O_4 , having magnetic permeability constants in the range of 0.5-35.5 (Rosensweig, 2006). The particles are large from a colloidal perspective, with particle diameters in the range of 1-100 microns. Continuous phases commonly employed include water, glycerin, mineral oil and silicon oil with viscosities in the range of 0.05-12 Pa.s, and magnetic permeability constants from 2.5-18 (Bica, 2006). To understand the response of MPA suspensions to the applied magnetic field, flow visualization experiments are performed to determine the state of structures formed in MPA suspensions under various, steady-state conditions. The experiments were performed by visually observing suspensions between two diamagnetic parallel plates. A diamagnetic substance has weak negative susceptibility which indicates that the direction of the induced magnetic dipole moment is opposite to the direction of the applied field (Bica, Liu, & Choi, 2013). This effect ensures that the diamagnetic plates do not enhance any magnetic field to the magnetized particles in the suspension.

Numerous machines and facilities use fluids as a working medium in a closed or open loop. Most of these operate in a turbulent flow regime, which produces friction loss much greater than laminar flow. To reduce capital investments by minimizing the system size and to lower operating costs by reducing energy loss, which are required for fluid circulation and delivery, it is very important to decrease flow friction in all fluid circulation and delivery systems. In the past, various materials such as polymers, asbestos, nylon, micelles, and particles were used as additive agents and mixed with working fluids through piping systems for investigation on friction reduction (Sreenivasan & White, 2000). Polymers existing in a curled chain shape, behave similarly to a multi-spring systems connected in series, which go through an expansion in a process of vortex stretching in turbulent flow. Polymer expansion absorbs turbulence energy and alters the extensional viscosity of the fluid (Yang, 2009). However, polymer macromolecules degrade quickly in practical applications, being cut to those of low molecular weight due to high stress levels existing in turbulent flow to lose their effectiveness. The degradation is permanent and hence they are useful for one-shot applications. Asbestos and nylon are fibers of long aspect ratio. They have been found to exhibit high resistance to vortex stretching arising in turbulent flow, which in turn can change the flow pattern (Hellsten, 2002). These fibers are not

practical for their long physical length involving possible gravitational settling and degradation with a performance inferior to polymers. The micelles form a rod-like shape and behave similarly to polymers and fibers under turbulent flow. At a critical stress, bonds within micelles are broken to lose effectiveness for friction reduction (Zhang, Schmidt, Talmon, & Zakin, 2005). However, the effective operating regime for micelles is restricted to a relatively narrow region close to the laminar flow. This shows that micelles are not applicable for a highly turbulent flow. The investigations for particles including ash, sand, and dust report less impressive performance than polymers or micelles (White & Mungal, 2008), making their application the least favorable.

In this paper, we investigated a new concept which utilizes magnetized particle agglomerates of ferromagnetic materials. MPA are believed to effectively reduce friction in turbulent pipe flow. MPA can enhance performance better than other materials for reducing friction and can be used reversibly in many cycles because of its strengths and flexibilities. We focused our investigation on the appropriate optimal operating ranges of pipe flow parameters such as particle size, mass concentration, intensity of initial magnetization, and Reynolds number.

2. Description of methods

The apparatus used to observe the behavior of the MPA suspension structure is schematically represented in Figure 1. The apparatus consists of two brass diamagnetic parallel plates. The bottom plate which is placed inside a plexiglas trough with dimensions of 0.7 cm x 38 cm x 202 cm. The top plate is mounted to a plexiglas fixture that is allowed to slide on two rails running the length of the trough. The dimensions of the top plate are 0.7 cm x 32 cm x 100 cm. The bottom plate is cut to make a small rectangular slit with dimensions of 0.5 mm x 10 mm. The top fixture is connected to a gear box through a pulley system and driven by a motor at constant velocities. The gear box contains a cylindrical iron core completely wound by a copper wire which is then connected to a 5 kV DC power supply. When the current passes through the copper wire, the magnetic field is generated at the magnitude of $H_0 = 4\pi ni / 10L$, downward from the top plate to the bottom plate, where n is the number of turns of the copper windings, i is the current in amperes, and L is the length of the cylindrical iron core.

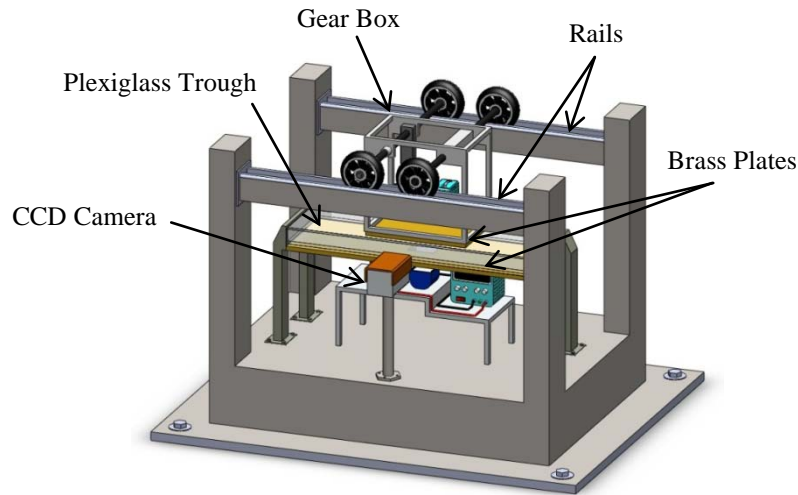


Figure 1 Schematic diagram of the flow visualization apparatus

The MPA suspensions described in this study consisted of ferromagnetic spheres, iron oxides Fe_2O_3 (type Gamma), suspended in glycerin. Before they were suspended in the glycerin, the ferromagnetic spheres were initially polarized with magnetic field strength of 1000 gauss (G). The overall diameter of ferromagnetic spheres in the experiments is about 20 microns. Experiments reported here were performed at a volume fraction of 2%. The MPA suspension structure was observed with a Sony XC-8500CE charge-coupled device (CCD). The CCD camera was mounted and directed to the suspension between two parallel plates, normal to both the direction of flow and the applied magnetic field. A spotlight was mounted at the bottom plate and was directed through a slit. The picture was magnified such that both parallel plates were in the viewing area on the screen, with the gap itself occupying 25-50% of the picture. Photographs were taken of selected frames, and are presented below.

The application of MPA was carried out by pipe flow experiments to investigate the reduction in flow friction. The efficiency of MPA in friction reduction in pipe flow can be calculated as

$$\% \text{ in friction reduction} = \frac{f_s - f_{MPA}}{f_s} \times 100$$

where f_s and f_{MPA} are friction factors in a given length of pipe for a pure solvent and friction factor

for the MPA solution at the same flow rate, respectively. The friction factor f , which represents the normalized pressure drop ΔP through the pipe length l or the normalized wall skin-friction shear stress τ_w , is defined by (Munson, Young, & Okiishi, 1998)

$$f = \frac{\Delta P}{(l/D)(\rho V^2/2)} = \frac{4\tau_w}{\rho V^2/2}$$

where D , V , and ρ are pipe diameter, average flow velocity and medium density, respectively.

In the fully-developed turbulent pipe flow, the eddy size ranges from the largest length scale of pipe diameter D down to the Kolmogorov microscale η , where $\eta/D \approx \text{Re}_D^{-3/4}$. Re_D is the Reynolds number based on the pipe diameter. Below the Kolmogorov length scale, the eddy energy is negligible owing to immediate viscous dissipation (Meneveau & Katz, 2000). For turbulent eddies larger than the Kolmogorov scale, some turbulent energy would be consumed to deform or realign the MPA chains while some may go into breaking apart the dipole-dipole contact (Meneveau & Katz, 2000). The dipole-dipole contact energy, E_{dd} or the energy required to break a bond between two magnetic particles is given by, $E_{dd} = \mu_0 M^2 V / 12$ where V is the volume of a dipole. In order for the particles to agglomerate, it is necessary that the dipole-dipole contact energy of MPA exceed the thermal energy

that would disperse them. We define γ as the ratio of these quantities (Socoliuc, Bica, & Vekas, 2003).

$$\gamma = \frac{E_{dd}}{kT} = \frac{\mu_0 M^{2/3} V}{12kT}$$

If the particles are spherical with equivalent diameter of σ and the fluid magnetization is linear with the imposed magnetic field H_0 ,

$$\gamma = \frac{\pi\sigma^3 \mu_0 \chi_m^{2/3} H_0^{2/3}}{72kT}$$

where $M = \chi_m H_0$. Thus, large particle and/or strong magnetic fields can enhance agglomeration by

making $\gamma = 1$. The shear force, τ_e contributed by the turbulent eddies can be approximated as

$$\tau_e \approx \mu \left(\frac{\varepsilon}{r^2} \right)^{1/5}$$

where ε is the energy dissipation rate per unit mass. Having the shear force inversely proportional to two fifth power of its size, small eddies can be effective sources of shear scission of the agglomerates as long as MPA are larger than the Kolmogorov scale (Lopez-Lopez, Kuzhir, Duran, & Bossis, 2010).

The pipe flow facility used to measure the friction reduction capability of MPA in turbulent pipe flow is shown in Figure 2.

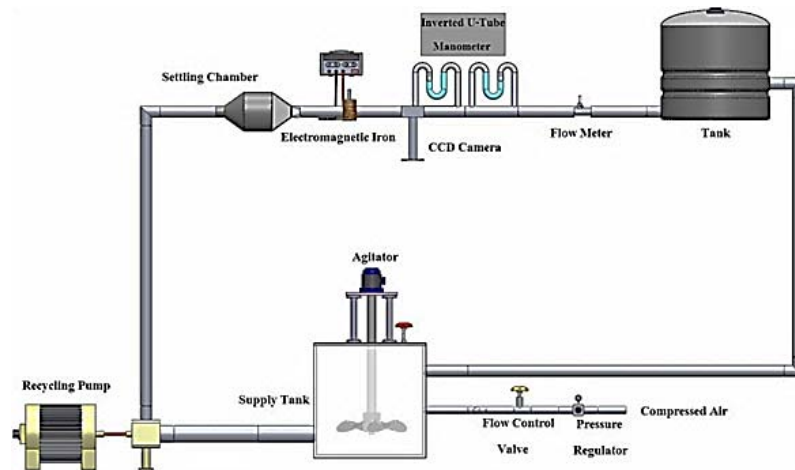


Figure 2 Schematic diagram of the pipe flow facility

The apparatus consists of supply tank containing magnetic particles suspended in water. Plastic pipe with inner diameter of 2.54 cm. is used to circulate the suspensions. The settling chamber contains honeycombs to straighten the flow in the same direction. As shown in Figure 3, the C-shaped electromagnetic iron is used as the in-line magnetic conditioner to provide the external magnetic field to MPA before entering the flow test zone. When the electric current goes through the copper wire that is wound around the C-shaped iron, the magnetic field is generated perpendicularly across the pipe and applied to the flow. The inverted U-tube manometer is used to measure the pressure drop and consequently, the friction reduction at the test zone.

In the experiment, iron oxides Fe_2O_3 particles were employed as additives. We divided the size ranges of particle into five groups: 19-38 nm, 1-30 microns, 30-50 microns, 50-70 microns,

and 70-90 microns. The particle mass concentration was made to range between 0% - 5%. Before suspending the magnetic particles into water, we initially polarized the particles in five different levels of intensity, ranging from 200 G to 1000 G at an increment of 200 G. The flow rates are categorized in five different Reynolds numbers, ranging from 20,000 to 100,000. After initial magnetization, the particles from each group were rapidly mixed with water by an agitator and immediately fed to a plastic pipe. The mixtures were circulated by using a centrifugal pump. Experiments consisted of two parts. The first experiment was done to preliminarily study the effectiveness of MPA in friction reduction, without application of an external in-line magnetic field. The second experiment included the effects of the in-line magnetic field by applying magnetic field at 500 G to the flow prior to the manometer section.

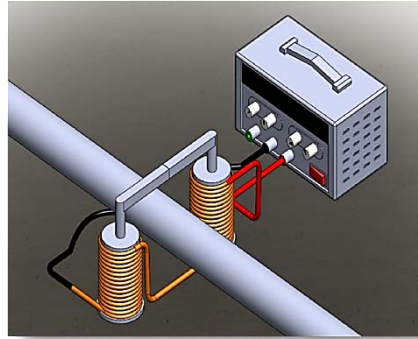


Figure 3 The C-shaped electromagnetic iron and the power supply

3. Results and discussion

Based on our experiments, we investigated the importance of external magnetic field strength in the initial polarization of the ferromagnetic materials and its effects on structure formation, the response of MPA structure to the shear stress, and time scale in structure formation. The polarization process or initial magnetization of these materials depended on their previous history. The maximum magnetic field that causes saturation for iron oxides is approximately 835 G. Thus, the four groups that were initially polarized from 200 G to 800 G are

below the saturation point. The last group that was initially polarized to 1000 G is over the saturation point. After removing all five groups from the initial magnetization field, we expected each group to retain their residual magnetization values in an increasing order.

Experiments began by placing suspension between two parallel plates within the plexiglas trough as shown in Figure 1. The static suspension of 1000 G initially magnetized particles without externally applied magnetic field is shown in Figure 4.



Figure 4 Static suspension of the particles of 1000 G initial magnetization with no external magnetic field

Fibrous skeletons were instantaneously formed for 1000 G magnetized-particles suspension when an external magnetic field of 500 G was

applied. Figures 5 and 6 show the fibrous skeletons or chain-like structures formed at 62 s and 120 s, respectively, after the magnetic field was applied.

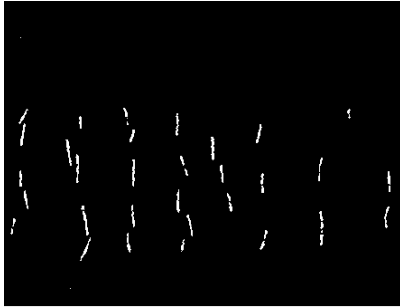


Figure 5 The process for fibrous skeleton formation for the 1000 G initially-magnetized particles suspension 62 s after the external magnetic field of 500 G was applied



Figure 6 Formation of static fibrous structure of 1000 G initially-magnetized particles suspension 120 s after the application of a 500 G magnetic field

The structure formed in two stages: formation of the fibrous skeleton or chain-like structure in a short period, followed by slight rearrangement within the fibers occurring in seconds. The application of the external magnetic field induced magnetic dipoles on the particles and aligned them with the applied field. The dipoles attracted one another head-to-tail, thus forming the fibrous aggregates. The interaction of the particulate columns with stresses can be observed by shearing a suspension to steady state at a specified shear rate. The transient time is approximately on the order of L^2/ν , where L is the gap width of parallel plates and ν is the kinematic viscosity of glycerin (Bossis, Khuzir, Lacic, & Volkova, 2003). The gap width is set to be 2 mm and the kinematic viscosity of glycerin at room temperature is approximately $1.19 \times 10^{-3} \text{ m}^2/\text{s}$, resulting in the transient time of 0.0034 s.

Since the transient time is very small, steady-state conditions were reached quickly.

Before performing each experiment at a specified shear rate, the magnetized particles suspension had to be in static conditions with the particulate columns aligned vertically between parallel plates. First, we showed the photographs of the suspensions in static conditions before shearing, followed by the photographs of the suspensions after shearing at a specified shear rate. Figure 7 shows the configuration of static fibrous aggregates in the 1000 G initially-magnetized particles suspension, before applying a shear rate of 0.5 s^{-1} . In Figure 1, the suspension is sheared with the top plate moving to the right. Figure 8 shows deformation of MPA strands at the shear rate of 0.5 s^{-1} . Most fibrous aggregates remained intact during shearing. If returned to the unstrained state, their structure appeared entirely unaffected.

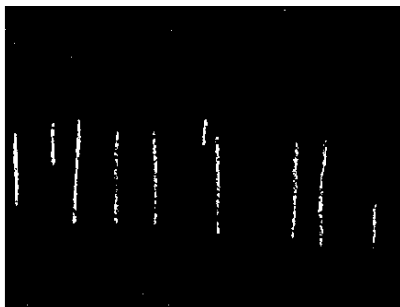


Figure 7 Configuration of static fibrous structure of the 1000 G initially-magnetized particles suspension before applying a shear rate of 0.5 s^{-1}

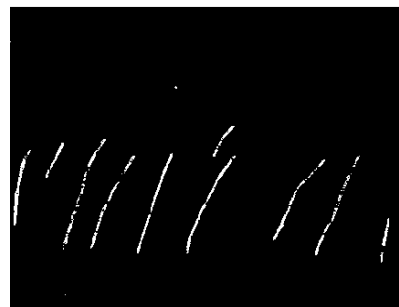


Figure 8 1000 G initially-magnetized particles suspension at a shear rate of 0.5 s^{-1} . Most fibers remain intact. Photographs was taken about 25 s after the top plate moved to the right

The configuration of static fibrous aggregates in 1000 G initially-magnetized particles suspension before applying a shear rate of 2 s^{-1} is shown in Figure 9. Figure 10 shows the rupture of fibrous structure in 1000 G initially-magnetized

particles suspension at a shear rate of 2 s^{-1} . The fibers break into smaller pieces while continuing to lean in the direction of the flow at an approximately constant angle conforming well to the shear displacement.

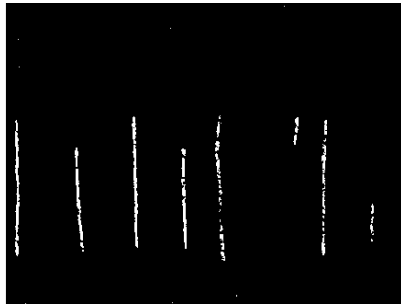


Figure 9 Configuration of static fibrous structure of the 1000 G initially-magnetized particles suspension before applying a shear rate of 2 s^{-1}

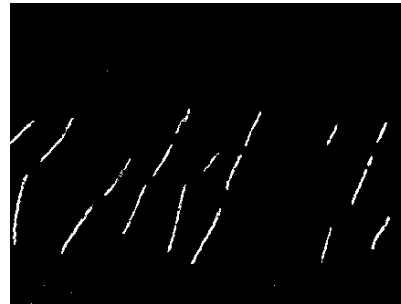


Figure 10 1000 G initially-magnetized particles suspension at a shear rate of 2 s^{-1} . The fibers break into smaller pieces. Photograph was taken about 20 s after the top plate moved to the right

In the pipe flow experiment, the goal was to find the optimal operating ranges for friction reduction among particle size, particle mass concentration, intensity of initial magnetization, and Reynolds number. First, the effect of particle mass concentration was tested. Particles of size 30-50 microns were chosen to be used in two experiments

at Reynolds number close to 60,000. The first experiment was performed without the in-line magnetic field. The second experiment was performed with the application of in-line magnetic field with the strength of 500 G. The particles were initially magnetized at 1000 G for both cases. The results are shown in Figure 11.

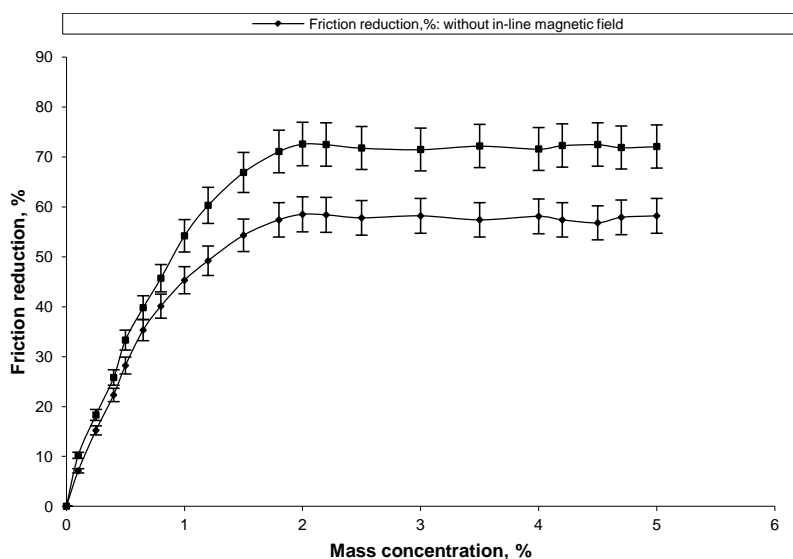


Figure 11 The effect of particle mass concentration on friction reduction for particle size 30-50 microns and at Reynolds number close to 60,000

The particle mass concentration exhibited clear effects on friction reduction. There was an increase in friction reduction with an increase in particle mass concentration to a point and the friction reduction efficiency becomes saturated. Therefore, increasing particle mass concentration after the saturation point does not influence the effectiveness in friction reduction. In the experiment, 2% mass concentration marks the saturation point where friction reduction is maximized. At 2% mass concentration, the friction reduction for the suspensions without the application of the in-line magnetic field is 58.5% and for the suspensions with the application of the in-line magnetic field is 72.6%. The error in Figure 11 is calculated to be $\pm 6\%$ due to

the measurement of the mass concentration and the fluctuation in the manometer when measuring the pressure drop across the test zone.

Next, we tested the effect of particle diameters on friction reduction. In each separate test, particles in the size ranges of 19-38 nm, 1-30 microns, 30-50 microns, 50-70 microns, and 70-90 microns were employed. For all the tests, the preconditioning in-line magnetic field of 500 G was applied and particle mass concentration was kept at 2%. As shown in Figure 12 for the results, all particle size ranges work well in reducing pipe flow friction especially for those in the range of 30-50 microns, 50-70 microns, and 70-90 microns.

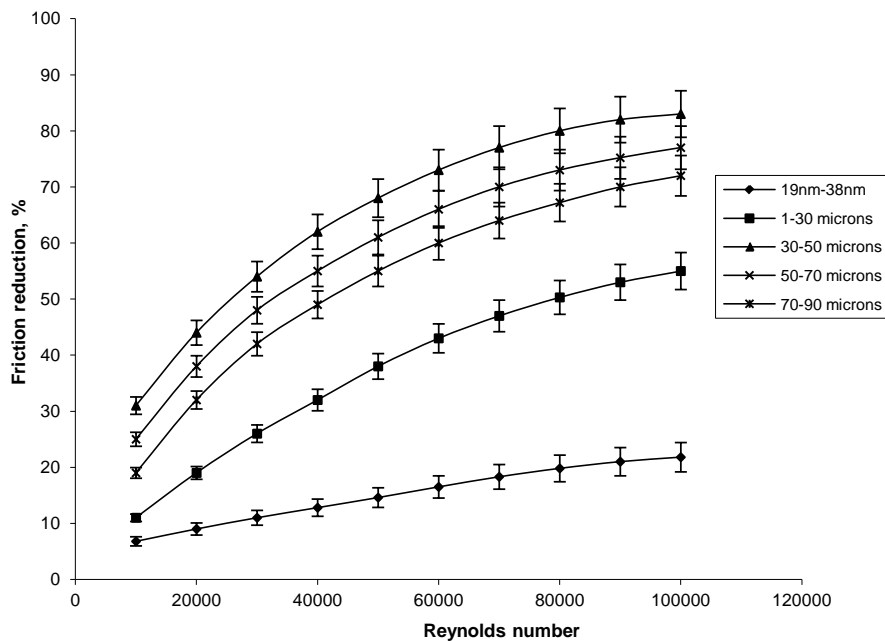


Figure 12 Effect of particle size and Reynolds number on friction reduction with the external in-line magnetic field of 500 G and mass concentration of 2%

The nanometer sized particles, comparable to the Kolmogorov scale, appear to have a small effect in friction reduction. Thus, the particles with diameters of 19-38 nm might not have any appreciable interaction with the major eddies in the turbulent process. Nano-particles, however, might have more pronounced effects in altering fluid rheological properties. The error in Figure 12 is

calculated to be $\pm 4\%$ due to the fluctuation in the manometer.

Figure 13 shows friction factor versus Reynolds number for particles with different magnitudes of initial magnetization, with diameter of 30-50 microns, at 2% mass concentration, and with the applied in-line magnetic field of 500 G. The error in this figure is calculated to be $\pm 4\%$.

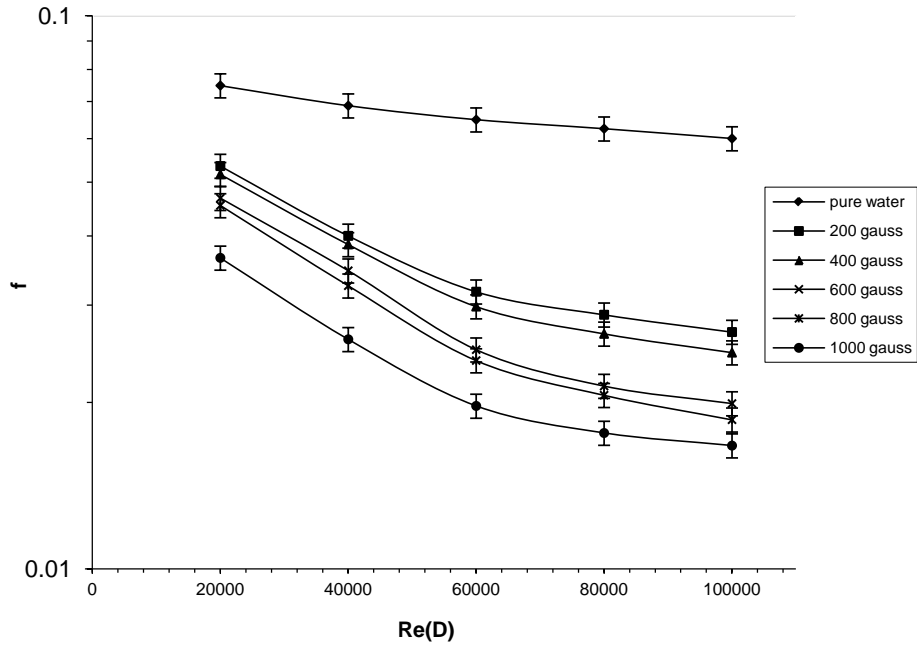


Figure 13 Friction factor versus Reynolds number for particles of diameter 30-50 microns, at 2% mass concentration, with the in-line magnetic field of 500 G

The errors arise in the pipe flow experiment due to the imperfection of the equipment in the pipe flow facility. The fluctuations in the flow meter that can affect the calculation in Reynolds number and the fluctuation in the manometer that causes for discrepancies in the reading are common examples. The external in-line magnetic field has an appreciable effect on the efficiency in friction reduction. The external field causes straightening and alignment of the strands of MPA in the direction of the applied field. The initial magnetization also plays an important role for the MPA to be effective. The magnetic particles that were initially magnetized with a magnetic field strength of 1000 G show significant effects in friction reduction.

4. Conclusion

In this paper, experimental observations of steady-state response of the MPA suspension structure were presented. The application of magnetic field induced magnetic dipoles on the particles, aligned with the applied field. The dipoles attracted one another, thus forming the fibrous aggregates. When strained past a critical value, all the fibers in the suspension ruptured almost simultaneously. At very small continuous rates of strain, the ruptured fibers continuously reformed

structures almost spanning the parallel plates, to be subsequently re-ruptured and reformed. At moderate shear rates, the structures underwent significant rearrangement. A fibrous mass remained closely attached to the lower plate during shear but the individual fibers were much less uniform and well-defined.

The application feasibility of MPA suspension was also investigated. Pipe flow experiments were performed using magnetized particles as additive agents to the flow medium. The initial attempt to study the effects of MPA in friction reduction showed good promise. Based on the current experiments of pipe flow, the appropriate operating ranges and parameters for friction reduction are: particles with diameter 30-50 microns, mass concentration of 2%, initial magnetization of 1000 G, externally applied magnetic field of 500 G, and at Reynolds number above 60,000. In the turbulent flow of a pipe, the friction drag or equivalently the axial pressure drop is governed mainly by the rate at which turbulent fluctuations transport axial momentum in the radial direction. We believe that the magnetized particle agglomerates behave similarly to the coiled spring system. The bonding forces of individual magnetic dipoles that consist of an MPA chain are properly

balanced with the viscous shear force of the turbulent flow. The MPA chains elongate and finally break as the low shear force increases to a critical value. The restoring force is still effective after breakage until the separation is far enough beyond the distance of influence. The MPA are continually effective through regeneration after scission, to form a stretched spring system within the distance of influence or recombining with other broken chains to re-break after recombination. These phenomena can absorb the highly-fluctuating turbulence energy near the pipe wall to reduce flow friction.

This investigation is based on the spherical particles. However, the fibrous particles of long aspect ratio may perform better in friction reduction. Special coating of particles for preventing sticking of columns may also assist performances. All these have to be investigated in the future.

5. References

- Bica, I. (2006). Electrical conductivity of magnetorheological suspensions based on iron microparticles and mineral oil in alternative magnetic field. *Journal of Industrial and Engineering Chemistry*, 12(5), 806-810.
- Bica, I., Liu, Y. D., & Choi, H. J. (2013). Physical characteristics of magnetorheological suspensions and their applications. *Journal of Industrial and Engineering Chemistry*, 19(2), 394-406. DOI:10.1016/j.jiec.2012.10.008
- Bossis, G., Khuzir, P., Laxis, S., & Volkova, O. (2003). Yield behavior of magnetorheological suspensions. *Journal of Magnetism and Magnetic Materials*, 258-259(March), 456-458. DOI:10.1016/S0304-8853(02)01096-X
- Di, Z., Chen, X., Pu, S., Hu, X., & Xia, Y. (2006). Magnetic-field-induced birefringence and particle agglomeration in magnetic fluids. *Applied Physics Letter*, 89, 211106. <http://dx.doi.org/10.1063/1.2392824>
- Hellsten, M. (2002). Drag-reducing surfactants. *Journal of Surfactants and Detergents*, 5(1), 65-70. DOI: 10.1007/s11743-002-0207-z
- Lopez-Lopez, M. T., Kuzhir, P., Duran, J. D. G., & Bossis, G. (2010). Normal stresses in a shear flow of magnetorheological suspensions: Viscoelastic versus Maxwell stresses. *Journal of Rheology*, 54, 146-157. <http://dx.doi.org/10.1122/1.3479043>
- Meneveau, C., & Katz, J. (2000). Scale invariance and turbulence models for large eddy simulation. *Annual Review of Fluid Mechanics*, 32, 1-32. DOI:10.1146/annurev.fluid.32.1.1
- Munson, B. R., Young, D. F., & Okiishi, T. H. (1998). *Fundamentals of Fluid Mechanics*. New York, USA: John Wiley & Sons, Inc.
- Rosensweig, R. E. (2006). Refrigeration aspects of magnetic particle suspensions. *International Journal of Refrigeration*, 29(8), 1250-1258. DOI:10.1016/j.ijrefrig.2006.03.021
- Socoliuc, V., Bica, D., & Vekas, L. (2003). Estimation of magnetic particle clustering in magnetic fluids from static magnetization experiments. *Journal of Colloid and Interface Science*, 264(1), 141-147. DOI:10.1016/S0021-9797(03)00426-0
- Sreenivasan, K. R., & White, C. M. (2000). The onset of drag reduction by dilute polymer additives and the maximum drag reduction asymptote. *Journal of Fluid Mechanics*, 409, 149-164.
- White, C. M., & Mungal, M. G. (2008). Mechanics and prediction of turbulent drag reduction with polymer additives. *Annual Review of Fluid Mechanics*, 40, 235-256. DOI:10.1146/annurev.fluid.40.111406.102156
- Yang, S. Q. (2009). Drag reduction in turbulent flow with polymer additives. *Journal of Fluid Engineering*, 131(5), 128-139.
- Zhang, Y., Schmidt, J., Talmon, Y., & Zakin, J.L. (2005). Co-solvent effects on drag reduction, rheological properties and micelle microstructures of cationic surfactants. *Journal of Colloid and Interface Science*, 286(2), 696-709. DOI:10.1016/j.jcis.2005.01.055